Color Me Intrigued: The Discovery of iPTF 16fnm, an SN 2002cx–like Object

A. A. Miller[1,2,3] , M. M. Kasliwal[3] , Y. Cao[4] , S. M. Adams[3], A. Goobar[5], S. Knežević[6] , R. R. Laher[7], R. Lunnan[3] ,
F. J. Masci[7] , P. E. Nugent[8,9] , D. A. Perley[10,11] , T. Petrushevska[5], R. M. Quimby[12,13] , U. D. Rebbapragada[14] ,
J. Sollerman[15] , F. Taddia[15], and S. R. Kulkarni[3]

[1] Center for Interdisciplinary Exploration and Research in Astrophysics (CIERA) and Department of Physics and Astronomy, Northwestern University, 2145 Sheridan Road, Evanston, IL 60208, USA; amiller@northwestern.edu
[2] The Adler Planetarium, Chicago, IL 60605, USA
[3] Division of Physics, Mathematics, and Astronomy, California Institute of Technology, Pasadena, CA 91125, USA
[4] eScience Institute and Astronomy Department, University of Washington, Seattle, WA 98195, USA
[5] The Oskar Klein Centre, Department of Physics, Stockholm University, AlbaNova, SE-106 91 Stockholm, Sweden
[6] Department of Particle Physics and Astrophysics, Weizmann Institute of Science, Rehovot 7610001, Israel
[7] Infrared Processing and Analysis Center, California Institute of Technology, Pasadena, CA 91125, USA
[8] Lawrence Berkeley National Laboratory, Berkeley, CA 94720, USA
[9] University of California—Berkeley, Berkeley, CA 94720, USA
[10] Dark Cosmology Centre, Niels Bohr Institute, University of Copenhagen, Juliane Maries Vej 30, DK-2100 København Ø, Denmark
[11] Liverpool John Moores University, Department of Astronomy, Liverpool, L3 5RF, UK
[12] Department of Astronomy, San Diego State University, San Diego, CA 92182, USA
[13] Kavli IPMU (WPI), UTIAS, The University of Tokyo, Kashiwa, Chiba 277-8583, Japan
[14] Jet Propulsion Laboratory, California Institute of Technology, Pasadena, CA 91109, USA
[15] The Oskar Klein Centre, Department of Astronomy, Stockholm University, AlbaNova, SE-106 91 Stockholm, Sweden
Received 2017 March 27; revised 2017 September 11; accepted 2017 September 11; published 2017 October 12

Abstract

Modern wide-field, optical time-domain surveys must solve a basic optimization problem: maximize the number of transient discoveries or minimize the follow-up needed for the new discoveries. Here, we describe the Color Me Intrigued experiment, the first from the intermediate Palomar Transient Factory (iPTF) to search for transients simultaneously in the g_{PTF} and R_{PTF} bands. During the course of this experiment, we discovered iPTF 16fnm, a new member of the 02cx-like subclass of Type Ia supernovae (SNe). iPTF 16fnm peaked at $M_{g_{PTF}} = -15.09 \pm 0.17$ mag, making it the second-least-luminous known SN Ia. iPTF 16fnm exhibits all the hallmarks of the 02cx-like class: (i) low luminosity at peak, (ii) low ejecta velocities, and (iii) a non-nebular spectrum several months after peak. Spectroscopically, iPTF 16fnm exhibits a striking resemblance to two other low-luminosity 02cx-like SNe: SN 2007qd and SN 2010ae. iPTF 16fnm and SN 2005hk decline at nearly the same rate, despite a 3 mag difference in brightness at peak. When considering the full subclass of 02cx-like SNe, we do not find evidence for a tight correlation between peak luminosity and decline rate in either the g' or r' band. We measure the relative rate of 02cx-like SNe to normal SNe Ia and find $r_{N_{02cx}/N_{Ia}} = 33^{+158}_{-25}\%$. We further examine the $g' - r'$ evolution of 02cx-like SNe and find that their unique color evolution can be used to separate them from 91bg-like and normal SNe Ia. This selection function will be especially important in the spectroscopically incomplete Zwicky Transient Facility/Large Synoptic Survey Telescope (LSST) era. Finally, we close by recommending that LSST periodically evaluate, and possibly update, its observing cadence to maximize transient science.

Key words: methods: observational – surveys – supernovae: general – supernovae: individual (SN 2002cx, SN 2005hk, iPTF 16fnm)

1. Introduction

1.1. The Transient Follow-up Problem

The proliferation of large-area optical detectors has led to a recent renaissance of time-domain astronomy and, in particular, the search for exotic transients. Over approximately the past decade, new surveys have dramatically increased the number of transients discovered on a nightly basis. These efforts will culminate with the Large Synoptic Survey Telescope (LSST) in the early 2020s, which will discover 2000 new supernovae (SNe) per night (Ivezić et al. 2008). Discovery is a small first step in improving our understanding of SNe. Detailed follow-up observations, either photometry spanning the ultraviolet, optical, and infrared (UVOIR) or spectra, are needed to reveal the nature of these explosions (see Filippenko 1997, for a review of SN spectra). Existing follow-up facilities are already taxed by the current rate of transient discovery, meaning that

the LSST-enabled two orders of magnitude increase in discovery rate poses a serious "follow-up problem." Namely, there will be substantially more known SNe than available resources to study each in detail.

Transient surveys are forced to balance the trade-off between transient discoveries and the need for follow-up resources. For a fixed exposure time, observing as wide an area as possible in a single filter will maximize the number of discoveries. Implicit in this strategy is the need for outside follow-up resources. If, on the other hand, follow-up resources are scarce or prohibitively expensive, a survey may choose to repeatedly observe the same fields in different passbands to obtain color information. This would, however, reduce the total number of transient discoveries. Both strategies are employed by modern surveys. Broadly speaking, shallow surveys tend to observe in a single filter (e.g., the All-Sky Automated Survey for Supernova (ASAS-SN; Shappee et al. 2014); the Palomar

Transient Factory (PTF; Law et al. 2009)), while deeper surveys sacrifice area for color (e.g., the Supernova Legacy Survey (SNLS; Astier et al. 2006); the Panoramic Survey Telescope and Rapid Response System 1 (PS1) Medium Deep Survey (MDS; Chambers et al. 2016), the Dark Energy Survey Supernova search (DES SN survey; Kessler et al. 2015)). The looming LSST "follow-up problem" has led to an increasing number of studies that consider only the photometric evolution of transients (e.g., Jones et al. 2017).

The intermediate Palomar Transient Factory (iPTF; Kulkarni 2013), which succeeded PTF,[16] is a time-domain survey consisting of a series of experiments. Like its predecessor, iPTF searched for transients using a single filter while obtaining two observations per field per night to reject asteroids from the transient-candidate stream. Here, we describe the Color Me Intrigued experiment from the final semester of iPTF. This experiment was the first from PTF/iPTF to search for transients with multiple filters, though this color information was achieved with no loss of survey area as the experiment still obtained two observations per field per night.

During the course of the Color Me Intrigued experiment, iPTF discovered a rare SN 2002cx-like object (hereafter 02cx-like SN), iPTF 16fnm, which we discuss in detail below.

1.2. Peculiar 02cx-like SNe

The discovery of an accelerating universe (Riess et al. 1998; Perlmutter et al. 1999) has led to numerous and extensive observational and theoretical studies into the nature of SNe Ia over the past two decades. Despite these efforts, a precise understanding of the nature and exact explosion mechanism for SN Ia progenitor systems is still unknown. While there is strong observational evidence that at least some SNe Ia come from white dwarf (WD) systems (e.g., Bloom et al. 2012a) and a general consensus that carbon/oxygen WDs give rise to SNe Ia, there is ambiguity in the mechanisms and scenarios that lead to explosion (e.g., Hillebrandt et al. 2013). A multitude of observational campaigns designed to capture large samples of SNe Ia for cosmological studies have also revealed several peculiar hydrogen-poor SNe (see Kasliwal 2012, and references therein). While these peculiar SNe retain many similarities to normal SNe Ia, their distinct properties allow for the possibility of more extreme or unusual WD progenitor scenarios.

To date, the most common subclass of peculiar SNe Ia are those similar to SN 2002cx (Li et al. 2003), of which there are now ∼25 known examples (e.g., Foley et al. 2013). The 02cx-like[17] class is characterized by low ejecta velocities (∼half normal SNe Ia) and low luminosities, ranging from $M \approx -19$ to -14 mag at peak. The distribution of host-galaxy morphologies for 02cx-like SNe is strongly skewed toward late-type hosts (e.g., Foley et al. 2013; White et al. 2015, and references therein), which may indicate massive star progenitors for this class (e.g., Valenti et al. 2009; Moriya et al. 2010). However, the maximum-light spectrum of SN 2008ha shows clear evidence for carbon/oxygen burning, providing a strong link

between 02cx-like SNe and WD progenitors (Foley et al. 2010).

While the sample of 02cx-like SNe is relatively small, they constitute a significant fraction of the total number of SNe Ia, ∼5%–30% (Li et al. 2011; Foley et al. 2013; White et al. 2015). Multiple efforts have been made to identify simple correlations between basic observational properties for the class (e.g., McClelland et al. 2010; Foley et al. 2013), in part to aid the identification of a likely progenitor scenario. Significant outliers exist (e.g., Narayan et al. 2011), however, and the emerging consensus is that 02cx-like SNe cannot be understood as a single-parameter family (Magee et al. 2017).

Pure deflagration models are often invoked to explain the heterogeneity of the 02cx-like class (e.g., Phillips et al. 2007), as they can naturally explain the wide range in peak luminosity. As a result, extensive theoretical consideration has been given to these models recently (e.g., Kromer et al. 2013; Fink et al. 2014), with the express purpose of understanding 02cx-like SNe. Recently, Magee et al. (2016) compared early spectroscopic observations of SN 2015H, an 02cx-like SN, to a deflagration model from Fink et al. (2014) and found good agreement. The model light curve evolves faster than the observations, though this may be reconciled with higher ejecta mass models (Magee et al. 2016). An interesting consequence of the pure deflagration models is that they do not completely unbind the WD, leaving a ∼1 $M_\odot$ bound remnant (Kromer et al. 2013).

Alternatively, Stritzinger et al. (2015) compared detailed observations of SN 2012Z, one of the most luminous members of the 02cx-like class, to pulsating delayed-detonation (PDD) models of exploding WDs. In particular, Stritzinger et al. observe potbellied [Fe II] profiles in the near-infrared at late times, which are an indication of high-density burning. Based on this observation and the direct comparison of model light curves and spectra, it is argued that SN 2012Z was a PDD explosion of a Chandrasekhar-mass WD and not a pure deflagration (Stritzinger et al. 2015).

While examining a large sample of low-velocity Type I SNe, it is argued in White et al. (2015) that 02cx-like SNe are the result of double-degenerate mergers. This may explain their observed heterogeneity, as the masses of merging WDs can vary significantly. White et al. prefer pure deflagration models as an explanation for 2002es-like SNe, a low-velocity subclass of SNe Ia that is distinct from the 02cx-like class (Ganeshalingam et al. 2012; Cao et al. 2016a). Moving forward, it is clear that additional 02cx-like SNe need to be found to distinguish between pure deflagrations, PDD explosions, double-degenerate mergers, and other possible mechanisms.

Here, we present the discovery of a new member of the 02cx-like class, iPTF 16fnm. iPTF 16fnm was discovered in the course of the iPTF *Color Me Intrigued* experiment, and it was first identified as a possible low-velocity SN with spectra from the Spectral Energy Distribution Machine[18] (SEDm; N. Blagorodnova et al. 2017, in preparation). Our spectroscopic follow-up campaign clearly identifies iPTF 16fnm as an 02cx-like SN, which we show is one of the faintest known members of the class. While Color Me Intrigued was designed to identify unusual transients based on their colors follow-up of iPTF 16fnm was first triggered as a transient in the local universe. Nevertheless, we

---

[16] The initial PTF survey was conducted from 2009 July through 2012 December. The iPTF survey was conducted from 2013 February through 2016 October. Finally, the iPTF extension was conducted from 2016 November through 2017 February.

[17] This subclass is sometimes alternatively referred to as SNe Iax (Foley et al. 2013).

[18] Documentation for SEDm is available at http://www.astro.caltech.edu/sedm/.

show that $g - r$ color curves are sufficient to discover 02cx-like SNe, like iPTF 16fnm.

2. Color Me Intrigued: The iPTF Two-filter Experiment

The iPTF survey has been organized as a series of time-domain experiments conducted with the Palomar 48-inch telescope (P48). Proposals for individual experiments are written by iPTF members and selected by an internal time allocation committee. The decision to focus on a single experiment at a time was made to minimize cadence interruptions and ensure that a specific science goal could be accomplished. Individual experiments were limited to two broadband filters, g_{PTF} and R_{PTF}, and 30 s exposure times, but otherwise free to select the targets and cadence of observations.

2.1. Two Filter or Not Two Filter?

Recognizing that the next-generation Zwicky Transient Facility (ZTF; Bellm 2016; Kulkarni 2016) would increase the discovery rate relative to PTF/iPTF by more than an order of magnitude, a ZTF pilot experiment was proposed to reduce the "follow-up problem" for the final semester of iPTF. In brief, the proposed experiment, titled Color Me Intrigued, would be the first by PTF/iPTF to survey simultaneously in the g_{PTF} and R_{PTF} filters. Even with fast spectroscopic resources (e.g., SEDm), ZTF transient discoveries will outpace follow-up capabilities. Adopting a two-filter strategy allows us to maximize the information content for each newly discovered transient, without compromising the overall survey area.

To reject asteroids as false positives in the search for transients, PTF/iPTF observes fields twice within the same night. Observation pairs separated by ∼0.5 hr can reject moving objects by requiring at least two co-spatial detections. Prior to Color Me Intrigued, these observations were obtained in a single filter. Color Me Intrigued retained the basic two observations per field per night strategy, but instead observed once in g_{PTF} and once in R_{PTF}. A main objective for Color Me Intrigued was to produce color curves, particularly at the epoch of discovery, for all newly found transients. These curves will, in turn, be used to build preliminary classification models for ZTF (e.g., Poznanski et al. 2002), which will enable a more efficient allocation of follow-up resources. Indeed, we later show that 02cx-like SNe can be reliably selected based on their color evolution (see Section 6).

This two-filter strategy was adopted as a ZTF pilot to address one major and one minor concern. The minor concern is that using two filters would somehow prevent the rejection of asteroids as nontransients. Given that asteroids are primarily rejected via their motion, however, the choice of filters should not hinder transient discovery. In practice, we found that the same-night, two-detection requirement rejected asteroids from the transient-candidate stream.

One of the primary science drivers for iPTF is the study of extremely young SNe. These discoveries critically rely on the successful maintenance of a 1-day search cadence, as upper limits ∼24 hr prior to the initial detection of a transient are an excellent indicator of youth (e.g., Gal-Yam et al. 2014; Cao et al. 2015, 2016a; Miller et al. 2017). The primary concern for the Color Me Intrigued strategy is that, despite a 1-day cadence, young transients may be missed owing to (i) extreme colors, (ii) differences in the depth of the g_{PTF} and R_{PTF} observations, or (iii) a combination of the two. For example, many young
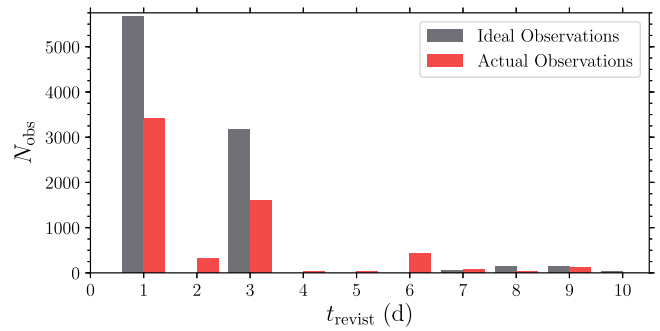

Figure 1. Revisit time, $t_{revisit}$, for all fields monitored during the Color Me Intrigued experiment. The designed, ideal cadence is shown in gray, while the true revisit times are shown in red. There is a small tail of observations with $t_{revisit} > 10$ days that is not shown for clarity.

transients are hot with blue $g_{PTF} - R_{PTF}$ colors. If a hot transient produces a faint g_{PTF} detection, then there may be no corresponding R_{PTF} detection, resulting in a nondetection. The same transient would have been discovered earlier with two g_{PTF}-band observations. Indeed, during Color Me Intrigued a handful of SNe were discovered only 1–6 days after their initial P48 detection, because those initial detections occurred in only a single filter. Additionally, iPTF g_{PTF}-band observations reach a flux limit that is a factor of ∼2 fainter than R_{PTF} band (Law et al. 2009). There is at least one relatively red SN ($g_{PTF} - R_{PTF} \approx 0.4$ mag) discovered after its initial detection owing to these differences in depth. Thus, one clear trade-off for adopting a two-filter strategy is that some transients are discovered at a later phase than they would be discovered by a single-filter search. A full systematic study of the biases introduced by the Color Me Intrigued strategy is beyond the scope of this paper and will be addressed in a future study (A. A. Miller et al. 2017, in preparation).

2.2. Observation Plan

The Color Me Intrigued experiment included 270 fields covering a total area of ∼1960 deg². The experiment was conducted for 3 months, from 2017 August 20 to November 10, using the ∼21 darkest nights during each lunation.[19] As a ZTF/LSST precursor, the experiment adopted a rolling cadence strategy. The 270 fields were split into three groups of 90. During each lunation, one group would be observed with a 1-day cadence, while the other two would be observed with a 3-day cadence. Therefore, 150 fields (90 with a 1-day cadence, and 60 with a 3-day cadence) would be observed each night, yielding 300 total observations. Over the course of the experiment each field was slated to be observed 42 times, though weather losses ultimately reduced this number.

As previously noted, maintaining a 1-day cadence is critical for the discovery of young SNe. In Figure 1 we summarize the ideal cadence for Color Me Intrigued (i.e., no loss of observing time) against the actual revisit time, $t_{revisit}$, for all fields monitored. The ideal cadence shows two prominent peaks at $t_{revisit} \approx 1$ and 3 days, with small peaks near ∼1 week due to Hα observations around full moon. The same peaks dominate the actual revisit times; however, only ∼60 and ∼50% of the planned 1-day and 3-day observations, respectively, occurred as scheduled. In other words, Color Me Intrigued was designed

[19] The ∼7 nights around full moon were allocated to the iPTF Census of the Local Universe Hα survey (Cook et al. 2017).
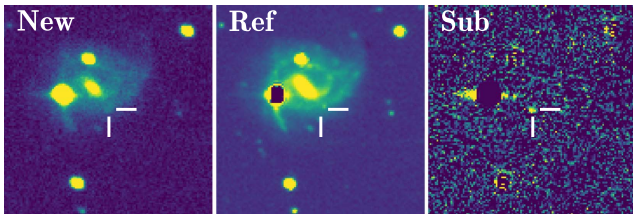
Figure 2. *R*-band discovery image of iPTF 16fnm showing the new, reference, and subtraction image from left to right. Images are shown on a linear scale, with the saturation levels selected to highlight faint structure in the host galaxy, UGC 00755. North is up and east to the left, and the images are centered on the SN position as indicated by the crosshairs, which are 10″ long.

to survey $90 \times 7.26 \deg^2 = 653.4 \deg^2 \text{ night}^{-1}$ with a 1-day cadence. Weather losses resulted in an effective 1-day cadence survey area of $405.8 \deg^2 \text{ night}^{-1}$. Similarly, $60 \times 7.26 \deg^2 = 435.6 \deg^2 \text{ night}^{-1}$ were to be observed with a 3-day cadence. Ultimately, the effective area of the 3-day search was $215.0 \deg^2 \text{ night}^{-1}$.

In closing, we note that scheduling constraints[20] prevented us from observing the first set of 1-day cadence fields during the third lunation of the experiment, 2017 October 19–November 10. These fields were replaced by 90 new fields, which were observed with a 3-day cadence. This change did not significantly affect the science output from Color Me Intrigued.

3. Observations of iPTF 16fnm

3.1. Discovery

iPTF 16fnm, located at $\alpha_{J2000} = 01^{h}12^{m}38^{s}.32$, $\delta_{J2000} = +38°30^{m}08''.8$, was first detected by iPTF at $R_{PTF} = 20.23 \pm 0.17 \text{ mag}$[21] on 2016 August 26.47 (UT dates are used throughout this paper). Following automated processing (Cao et al. 2016b; Masci et al. 2017) and the use of machine-learning software that separates real transients from image subtraction artifacts, known as `realbogus` (Bloom et al. 2012b; Brink et al. 2013; Masci et al. 2017), the candidate was manually saved and internally designated iPTF 16fnm. The discovery image of iPTF 16fnm is shown in Figure 2.

The iPTF 16fnm host galaxy, UGC 00755, has a redshift $z_{host} = 0.02153$ (Wegner et al. 1993). Adopting $H_0 = 73 \text{ km s}^{-1} \text{ Mpc}^{-1}$ and correcting for Virgo infall, this redshift corresponds to a distance $d = 90.5 \pm 6.3 \text{ Mpc}$ and distance modulus $\mu = 34.78 \pm 0.15 \text{ mag}$ (Mould et al. 2000). Thus, at the time of discovery iPTF 16fnm had an absolute magnitude $M_{R_{PTF}} \approx -14.5 \text{ mag}$. The light curve peaked ~3 days later at $M \approx -15 \text{ mag}$ in both the g_{PTF} and R_{PTF} filters, suggesting that iPTF 16fnm may be a "gap" transient (see Kasliwal 2011, 2012, and references therein).

The first spectrum of iPTF 16fnm was obtained on 2016 September 03.25 with the SEDm integral field unit spectrograph (Ben-Ami et al. 2012; N. Blagorodnova et al. 2017, in preparation) on the Palomar 60-inch telescope (P60).

---

[21] Photometry for iPTF 16fnm is reported in the g_{PTF} and R_{PTF} filters throughout, which are similar to the SDSS g' and r' filters, respectively (see Ofek et al. 2012, for details on PTF calibration). The correction from the g_{PTF} and R_{PTF} filters to SDSS g' and r' requires knowledge of the intrinsic source color (see Equations (1) and (2) in Ofek et al. 2012). 02cx-like SNe do not follow a standard spectral evolution, so the color terms for iPTF 16fnm are unknown.

Table 1
iPTF 16fnm P48 Photometry

HJD −2,457,600	Mag.[a]	σ_{mag}
	g_{PTF}	
27.008	20.04	0.26
30.002	19.80	0.10
32.990	19.88	0.11
35.998	20.20	0.13
38.992	20.34	0.17
41.964	20.89	0.29
42.951	20.99	0.27
56.972	>20.10	…
62.963	>20.50	…
65.962	>20.71	…
65.963	>20.60	…
68.951	>20.42	…
	R_{PTF}	
14.863	>20.30	…
14.905	>20.67	…
14.948	>20.74	…
15.833	>20.17	…
15.863	>20.26	…
15.892	>20.51	…
26.971	20.23	0.17
29.964	19.81	0.13
32.954	19.95	0.13
35.964	19.91	0.10
38.960	20.04	0.10
41.009	20.08	0.12
41.022	20.16	0.13
42.002	20.11	0.14
42.986	20.19	0.14
43.998	19.96	0.10
44.019	20.27	0.14
57.008	20.74	0.28
63.001	>20.63	…
66.001	>20.59	…
66.002	>20.33	…
68.991	>20.39	…

Note.
[a] Observed magnitude, not corrected for Galactic extinction. 5σ upper limits are reported for epochs where iPTF 16fnm is not detected.

This spectrum showed low-velocity Si II absorption, which, in conjunction with the relatively faint absolute magnitude, suggested that iPTF 16fnm may be a subluminous 02cx-like SN, similar to SN 2008ha (Foley et al. 2009). Subsequent spectra obtained with larger-aperture telescopes confirmed this initial classification.

3.2. Photometry

Photometric observations of iPTF 16fnm were conducted in the g_{PTF} and R_{PTF} bands using the PTF camera (Law et al. 2009) on the P48. The brightness of iPTF 16fnm was measured following image subtraction via point-spread function (PSF) photometry with the `PTFIDE` software package (Masci et al. 2017). These measurements are summarized in Table 1 and shown in Figure 3. We only consider the SNe detected in epochs where the signal-to-noise ratio (S/N) is ⩾3, while we otherwise conservatively report 5σ upper limits.
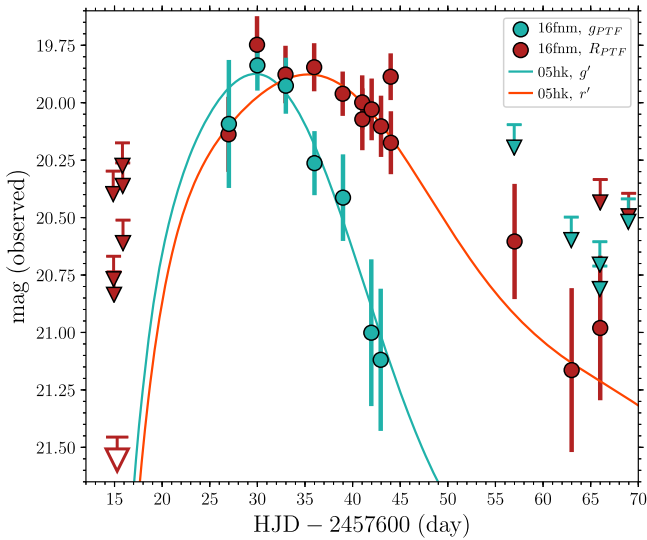
Figure 3. P48 light curves showing the evolution of iPTF 16fnm. Teal and crimson circles show detections in the g_{PTF} and R_{PTF} bands, respectively. 5σ upper limits are shown with downward-pointing arrows. The open downward-pointing arrow shows the 5σ upper limit from combining the 6 epochs taken ~11–12 days prior to discovery. The solid teal and red-orange lines show polynomial fits to the g' and r' filter observations, respectively, of SN 2005hk (Phillips et al. 2007). The curves have been shifted to align the time and brightness of maximum in g band for both SNe and stretched to match the redshift of iPTF 16fnm. The general agreement between the two suggests that the rise time for iPTF 16fnm is similar to that for SN 2005hk, ~15 days.

We determine the time of and brightness at maximum for iPTF 16fnm via second-order polynomial fits to the epochs when iPTF 16fnm was detected. From these fits we find that iPTF 16fnm peaked on HJD $2,457,629.8 \pm 2.0$ and $2,457,632.8 \pm 4.8$ at 19.87 ± 0.07 mag and 19.88 ± 0.05 mag in the g_{PTF} and R_{PTF} bands, respectively. These measurements represent the observed maxima of iPTF 16fnm and have not been corrected for Milky Way or host-galaxy extinction. 02cx-like SNe do not follow a standard color evolution, meaning that host-galaxy extinction cannot be inferred from photometry alone. We do not detect narrow Na I D at the redshift of UGC 00755 in any of our spectra, and therefore we assume that host-galaxy extinction is negligible. This assumption is supported by the observed blue color of iPTF 16fnm at peak.

Adopting the distance modulus to UGC 00755 and correcting for foreground Galactic extinction ($A_g = 0.178$ mag, $A_r = 0.123$ mag; Schlafly & Finkbeiner 2011), we find that iPTF 16fnm peaked at $M_{g_{PTF}} = -15.09 \pm 0.17$ mag and $M_{R_{PTF}} = -15.02 \pm 0.16$ mag, under the assumption of no local host extinction.

We cannot place strong observational constraints on the rise time of iPTF 16fnm: prior to its initial detection, iPTF had not observed this field for ~12 days (see Figure 3). If we combine the forced-PSF flux measurements from the 6 epochs taken between HJD $2,457,614$ and $2,457,616$, we derive a more constraining inverse-variance-weighted upper limit of $R_{PTF} > 21.46$ mag on HJD $2,457,615.3$. This deeper nondetection suggests that the rest-frame rise time of iPTF 16fnm is <17.2 days in the R band. Further constraints on the rise time are available by comparing iPTF 16fnm and SN 2005hk, the 02cx-like SN with the best observational constraints on the time of explosion (Phillips et al. 2007). Figure 3 shows polynomial fits to the g'- and r'-band light curves of SN 2005hk, shifted to match the time and brightness of

iPTF 16fnm in the g_{PTF} band and stretched to match the redshift of iPTF 16fnm. Formally, no further stretch factor is required to provide an excellent match between SN 2005hk and iPTF 16fnm, as seen in Figure 3. Assuming that SN 2005hk and iPTF 16fnm have similar compositions, opacities, and temperatures, which is reasonable based on the spectral similarities of the two SNe, the rise time of iPTF 16fnm is ~15 days (Phillips et al. 2007), consistent with our R_{PTF} observational constraints above.

Furthermore, a gap in our observations between ~13 and 27 days after g-band maximum makes it difficult to properly measure the decline rate of iPTF 16fnm. If we adopt the same quadratic fit used to determine the time of g-band maximum to estimate the SN brightness beyond +13 days after maximum, then iPTF 16fnm declined by 1.75 ± 0.46 mag in the g_{PTF} band after 15 days in its rest frame. Using the same similarity arguments about SN 2005hk from above, then we would expect the two SNe to feature similar declines, meaning for iPTF 16fnm $\Delta m_{15}(B) \approx 1.6$ mag, as was found for SN 2005hk (Phillips et al. 2007).

3.3. Spectroscopy

Optical spectra of iPTF 16fnm were obtained on 2016 September 03.3 and 2016 September 07.3 with the SEDm on the Palomar 60-inch telescope (P60). Additional spectra were obtained on 2016 September 03.4 with the Double Beam Spectrograph (DBSP; Oke et al. 1995) on the Palomar 200-inch telescope (P200), on 2016 September 06.1 and September 10.1 with the Andalucia Faint Object Spectrograph and Camera (ALFOSC) on the Nordic Optical Telescope (NOT), and on 2016 September 30.5 and November 28.4 with the low-resolution imaging spectrometer (LRIS; Oke & Gunn 1982) on the Keck I 10 m telescope. All spectra were extracted and calibrated using standard procedures. The sequence of iPTF 16fnm spectra is shown in Figure 4. A log of our spectroscopic observations is presented in Table 2.[22]

iPTF 16fnm shows the hallmark features of 02cx-like SNe: low-velocity lines of intermediate-mass and Fe-group elements. In our earliest spectroscopic observations, taken within a week of g_{PTF}-band maximum, Si II $\lambda6335$ shows an expansion velocity of only ~2000 km s^{-1}. Other relatively unblended lines, such as Ca H&K, Fe II $\lambda4555$, and O I $\lambda7774$, show expansion speeds of ~3200 km s^{-1}.

The late-time spectra of iPTF 16fnm resemble the evolution of other 02cx-like SNe. For example, like SN 2008ha (see Foley et al. 2009), absorption from Fe II $\lambda4555$ is prominent (pseudo-equivalent width [pEW] ≈ 100 Å) more than a month after maximum. Additionally, a strong P Cygni profile at ~5800 Å, possibly associated with Na I D, which would correspond to $v \approx 3000$ km s^{-1}, persists through our +89-day spectrum. Similarly, SN 2008ha shows similar absorption at $v \approx 2000$ km s^{-1} through +62 days, while SN 2002cx shows the same P Cygni feature ($v \approx 1500$ km s^{-1}) at +277 days. Finally, we note that our final spectrum of iPTF 16fnm shows weak [Ca II] $\lambda\lambda7291$, 7323 emission (EW ≈ -20 Å), which is similar to what is observed in SN 2002cx at very late times (Jha et al. 2006). The optical spectra of SN 2008ha, on the other hand, are completely dominated by [Ca II] (EW ≈ -500 Å) at a similar epoch, +65 days (Valenti et al. 2009).

---

[22] Our iPTF 16fnm spectra will be publicly released via WISeREP (Yaron & Gal-Yam 2012) following paper acceptance.
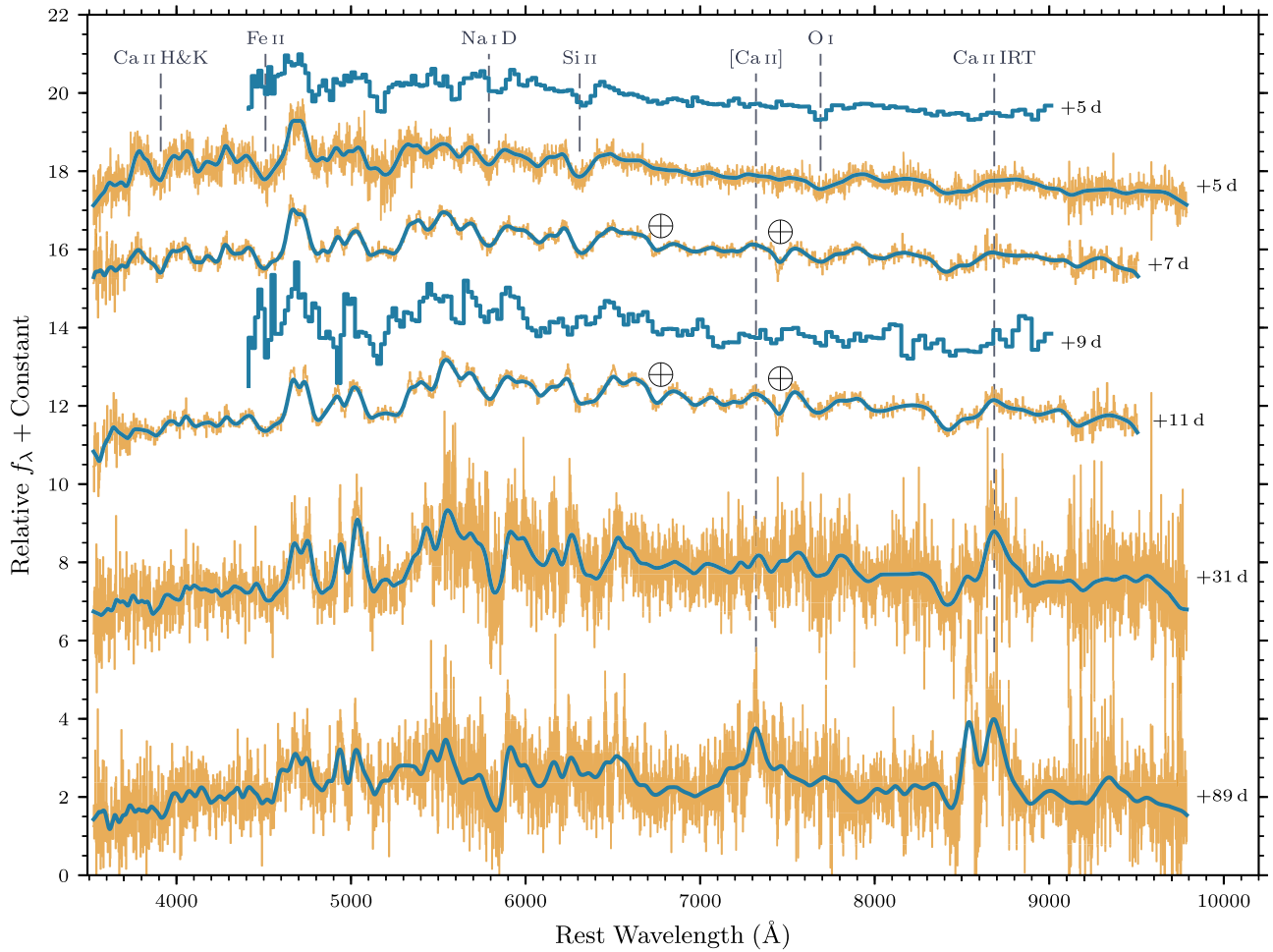
Figure 4. Spectral evolution of iPTF 16fnm. The spectra are labeled with their rest-frame phase relative to the observed g_{PTF}-band maximum. The non-SEDm spectra are shown in orange, while the solid blue lines show the same spectra convolved with a Gaussian filter with FWHM = 2500 km s^{-1}. SEDm spectra (+5 and +9) are shown as solid blue lines, and the low-S/N portion ($\lambda < 4500$ Å) is not shown for clarity. Characteristic features of 02cx-like SNe discussed in the text are labeled with vertical dashed lines.

Table 2
Log of Spectroscopic Observations

t^{a} (days)	UT Date	Instrument[b]	Range (Å)	Exp.[c] (s)	Air Mass
4.9	2016 Sep 03.25	SEDm	3806–9187	2700	1.51
5.0	2016 Sep 03.36	DBSP	3101–10236	1200	1.07
7.7	2016 Sep 06.13	ALFOSC	3427–9714	4800	1.02
8.8	2016 Sep 07.25	SEDm	3807–9187	2700	1.46
11.5	2016 Sep 10.06	ALFOSC	3556–9712	4800	1.10
31.5	2016 Sep 30.53	LRIS	3071–10297	975	1.14
89.1	2016 Nov 28.37	LRIS	3057–10276	3370	1.14

Notes.
[a] Age in rest-frame days relative to the observed g_{PTF} maximum on 2016-08-29.298.
[b] SEDm: Spectral Energy Distribution Machine on the Palomar 60-inch telescope. DBSP: Double Beam Spectrograph on the 200-inch Palomar Hale Telescope. ALFOSC: Andalucia Faint Object Spectrograph and Camera on the 2.6 m Nordic Optical Telescope. LRIS: low-resolution imaging spectrograph on the 10 m Keck I telescope.
[c] Exposure time.

We measure the expansion velocities for different species in iPTF 16fnm by tracking the wavelength of the minimum for each feature, as shown in Figure 5. The measurements are made
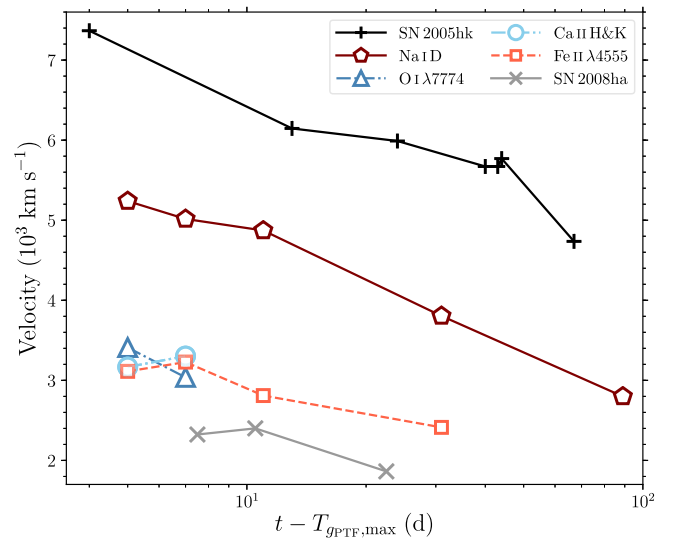

Figure 5. Velocity evolution of the absorption minimum of Ca H&K (circles), Fe II $\lambda4555$ (squares), Na I D (pentagons), and O I $\lambda7774$ (triangles) for iPTF 16fnm traced by the minimum of absorption. Also shown is the velocity evolution of SN 2005hk (plus signs, as traced by Fe II $\lambda4555$) and SN 2008ha (crosses, as traced by O I $\lambda7774$). The spectra for SN 2005hk and SN 2008ha are taken from Phillips et al. (2007) and Foley et al. (2009), respectively. iPTF 16fnm is clearly intermediate between SN 2005hk and SN 2008ha. For iPTF 16fnm the Na I D doublet may be contaminated by other features affecting our velocity measurements.
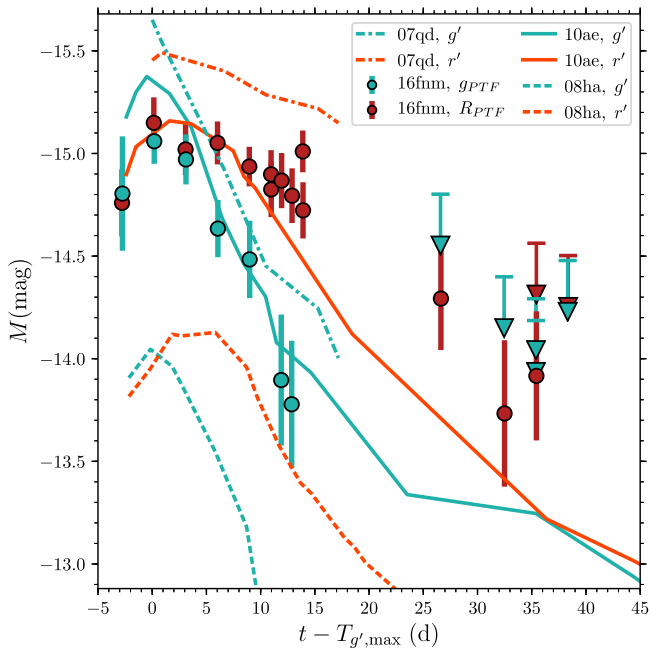
Figure 6. Photometric evolution of the faintest members of the 02cx-like class in the g' and r' filters. From brightest to faintest they are SN 2007qd, SN 2010ae, iPTF 16fnm, and SN 2008ha. These SNe all feature fast declines in the g' band, $\Delta m_{15}(g) \gtrsim 1.2$ mag. SN 2007qd and iPTF 16fnm, on the other hand, exhibit relatively slow declines in the r' filter.

following a convolution of the spectra with a Gaussian kernel with FWHM = 2000 km s^{-1}. Blending and the relatively low S/N of the spectra make it challenging to track the evolution of individual lines more than 10 days after g_{PTF}-band maximum. The Fe II λ4555 feature shows a modest decrease of only ~700 km s^{-1} from +5 to +31 days. At +5 days after maximum the Na I D feature exhibits significantly faster speeds of ~5200 km s^{-1}, decreasing to ~2800 km s^{-1} at +89 days. The higher velocities for this line indicate that our measurement may be contaminated by other features. Taken together, these lines demonstrate that iPTF 16fnm has a velocity structure that is intermediate between SN 2005hk, with typical velocities of ~7000 km s^{-1} (Phillips et al. 2007), and SN 2008ha, with typical velocities of ~2000 km s^{-1} (Foley et al. 2009; Valenti et al. 2009).

4. Comparison to Other Subluminous 02cx-like SNe

We compare the photometric evolution of iPTF 16fnm to other subluminous 02cx-like SNe in Figure 6. The comparison SNe are SN 2007qd (McClelland et al. 2010), SN 2010ae (Stritzinger et al. 2014), and SN 2008ha (Stritzinger et al. 2014), all low-luminosity 02cx-like SNe with g'- and r'-band photometric coverage.[23] Each light curve in Figure 6 has been corrected for foreground Galactic extinction using the Schlafly & Finkbeiner (2011) updates to the Schlegel et al. (1998) reddening maps. SN 2010ae has been further corrected for a host-galaxy reddening of $E(B - V)_{\mathrm{host}} = 0.50$ mag (Stritzinger et al. 2014; Foley et al. 2013). The light curves have been shifted to align the time of g'-band maximum, where we have assumed that the first detection of SN 2007qd corresponds to g'-band maximum (see McClelland et al. 2010, for further details). We adopt distance moduli of 36.23,

30.44, and 31.64 mag for SN 2007qd, SN 2010ae, and SN 2008ha, respectively, which are corrected for Virgo infall (Mould et al. 2000) and assume $H_0 = 73$ km s^{-1} Mpc^{-1}. No K- or S-corrections have been applied.

Figure 6 shows that iPTF 16fnm is generally similar to SN 2010ae and SN 2007qd. In particular, all three SNe are of comparable brightness at peak (-15 mag $\lesssim M \lesssim -15.5$ mag) and exhibit a fast decline ($\Delta m_{15}(g) \approx 1.3$ mag). SN 2008ha, on the other hand, is >1 mag fainter than the other SNe. Interestingly, both iPTF 16fnm and SN 2007qd exhibit a slow decline in the R_{PTF}/r' band, evolving from $g' - r' \approx 0.1$ mag near peak to $g' - r' \approx 0.9$ mag at $t \approx 15$ days.

We compare the same four SNe, as well as SN 2005hk, at similar epochs, $t \approx +4$ to $+10$ days, in Figure 7. The spectra are ordered top to bottom from the most luminous to least luminous, though note that changes in host-galaxy reddening could rearrange the middle three spectra. From Figure 7 it is clear that SN 2005hk has the highest velocity features (~6000 km s^{-1} at +10 days as traced by Fe II λ4555), while SN 2007qd, SN 2010ae, and iPTF 16fnm all have similar velocities (~3000 km s^{-1} at +10 days), and SN 2008ha has the lowest velocity signatures (~2500 km s^{-1} at +10 days).[24] The overall similarity of SN 2007qd, SN 2010ae, and iPTF 16fnm is striking. These three SNe are clearly closely related with similar velocities and ejecta composition, which is dominated by intermediate-mass elements. While the 02cx class as a whole exhibits great diversity, SN 2007qd, SN 2010ae, and iPTF 16fnm feature nearly identical spectra and photometric evolution, suggesting that they had similar progenitors or explosion mechanisms.

5. Results

While 02cx-like SNe exhibit a large range in luminosity (SN 2008ha and SN 2009kr are separated by ~2 orders of magnitude), their general similarity to normal SNe Ia has led many to search for correlated observational properties to unify the class. While the precise details of the explosion mechanism are debated, the observational consensus points to WD progenitors for 02cx-like SNe (see, e.g., Foley et al. 2013; Stritzinger et al. 2015; Magee et al. 2017). Thus, it may be the case that 02cx-like SNe are a single-parameter family, much like SNe Ia, whose evolution is largely controlled by the amount of ^{56}Ni synthesized during explosion (Mazzali et al. 2007).

Using the first four known 02cx-like SNe, SN 2002cx, SN 2005hk, SN 2007qd, and SN 2008ha, a potential correlation between absolute magnitude and ejecta velocity, whereby more luminous events also have faster ejecta, was identified in McClelland et al. (2010). The subsequent discovery of SN 2009ku (Narayan et al. 2011), which had extremely low velocities, like SN 2008ha, while also being the most luminous member of the class, posed a significant challenge to this correlation. While an increased sample of 02cx-like SNe shows a general correlation between ejecta velocity and luminosity (see Figure 20 in Foley et al. 2013), SN 2009ku remains a significant outlier.

---

[23] We remind the reader that iPTF 16fnm was observed in the g_{PTF} and R_{PTF} filters, which are similar to SDSS g' and r' (see Ofek et al. 2012, for the filter transformations).

[24] While these five SNe show an apparent correlation between absolute magnitude and velocity, SN 2009ku, the only 02cx-like SN with velocities as low as SN 2008ha is also the most luminous 02cx-like SN (Narayan et al. 2011).
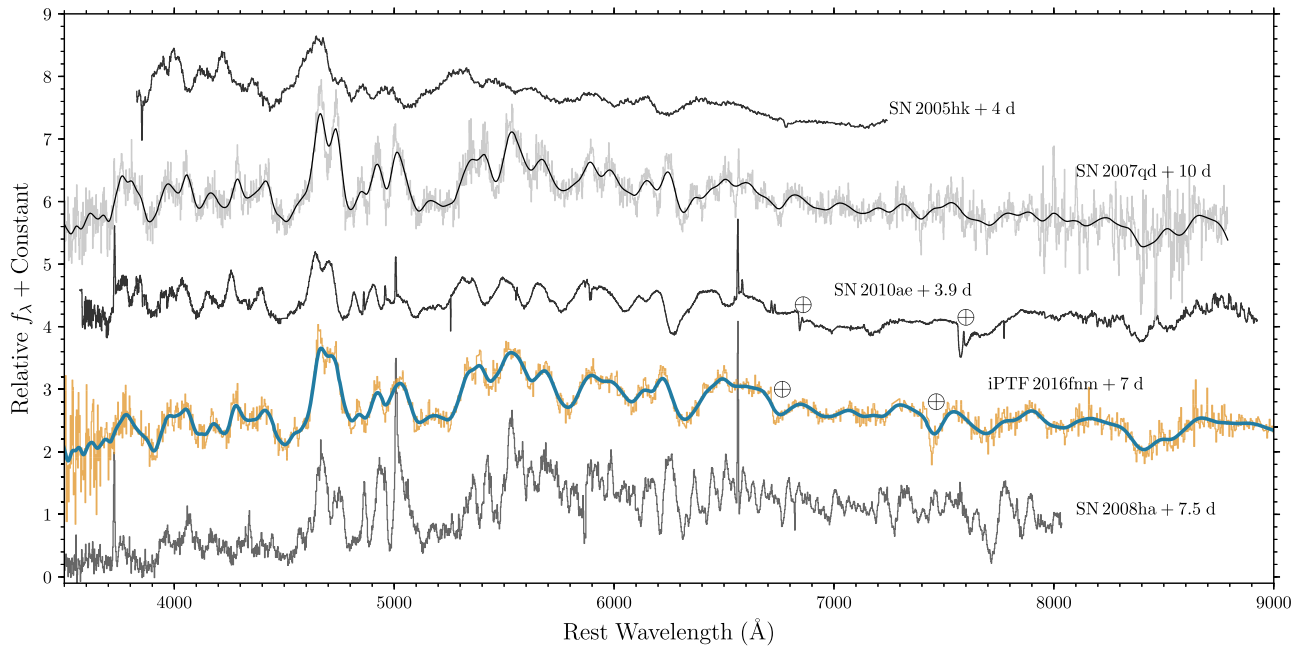
Figure 7. Spectral comparisons of iPTF 16fnm to other subluminous 02cx-like SNe. The spectra are labeled with their rest-frame phase relative to B- or g'-band maximum. SN 2007qd and iPTF 16fnm are also shown following convolution with an FWHM = 2500 km s^{-1} Gaussian kernel. From top to bottom, the spectra are SN 2005hk (Phillips et al. 2007), SN 2007qd (McClelland et al. 2010), SN 2010ae (Stritzinger et al. 2014), iPTF 16fnm, and SN 2008ha (Foley et al. 2009). SN 2005hk is a prototypical 02cx-like SN, while SN 2007qd and SN 2010ae, like iPTF 16fnm, were fainter at the time of maximum brightness with lower expansion velocities. SN 2008ha is the faintest member of the 02cx-like class.

5.1. The Luminosity–Decline Relation for 02cx-like SNe

Many studies have examined whether 02cx-like SNe follow their own Phillips relation, similar to SNe Ia, whereby more luminous SNe Ia also have broader light-curve shapes (Phillips 1993). Using a sample of 13 02cx-like SNe, evidence for an anticorrelation between M_V and $\Delta m_{15}(V)$ is presented in Foley et al. (2013). The V-band $M-\Delta m_{15}$ relation presented in Foley et al. (2013) exhibited significant scatter, well in excess of that found for normal SNe Ia. Furthermore, the sample in Foley et al. (2013) excludes SN 2007qd, which declined at a similar rate to that of SN 2005hk, despite being ∼2.5 mag fainter at peak.[25]

iPTF 16fnm provides additional evidence for the lack of a simple $M-\Delta m_{15}$ relation for 02cx-like SNe. In particular, Figure 3 shows that iPTF 16fnm declined at a nearly identical rate to SN 2005hk, which peaked at $M_{g'} = -18.08 \pm 0.25$ mag (Stritzinger et al. 2015), 3 mag brighter than iPTF 16fnm, $M_{g_{PTF}} = -15.08 \pm 0.17$ mag. To further illustrate this point, we update Figure 10 from White et al. (2015) to include iPTF 16fnm, as shown in Figure 8. For 02cx-like SNe with available g' observations, we additionally include estimates of $M_{g'}$ and $\Delta m_{15}(g')$ using the same procedure adopted in White et al. (2015). Even if SN 2007qd is excluded from the sample, iPTF 16fnm stands out as a strong outlier for any $M-\Delta m_{15}$ relation in the r'/R_{PTF} band. Examining those sources with g' observations, Figure 8 shows weak evidence for an $M-\Delta m_{15}$ relation, though the scatter is extremely large. As already noted, SN 2005hk and iPTF 16fnm exhibit similar decline rates but differ
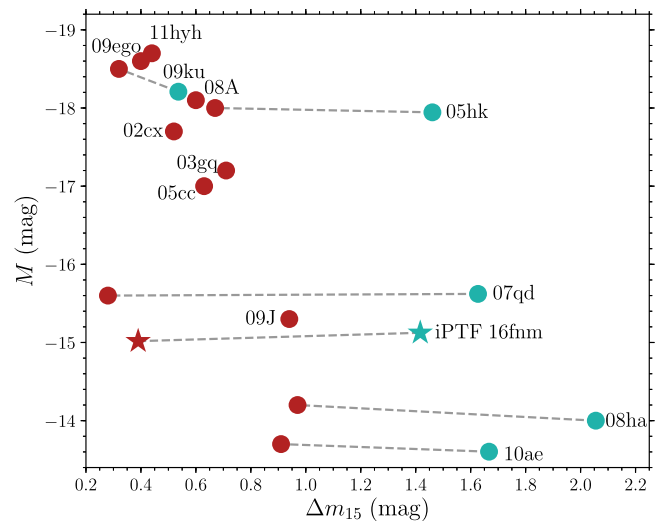

Figure 8. Absolute magnitude vs. Δm_{15}, in both the r' (shown in crimson) and g' bands (teal), for 02cx-like SNe, adapted from White et al. (2015). The dashed gray lines connect SNe for which both r' and g' observations are available. Note that, following White et al. (2015), we have not corrected M for host-galaxy extinction, which is why SN 2010ae is fainter than SN 2008ha in this figure. In the r' band most 02cx-like SNe lie along a high-scatter sequence, though SN 2007qd and iPTF 16fnm are clear outliers. Similarly, g'-band observations of 02cx-like SNe also show weak evidence for a simple $M-\Delta m_{15}$ relation.

by ∼3 mag at peak. Furthermore, SN 2005hk and SN 2009ku both peak at $M_{g'} \approx -18$ mag, yet their $\Delta m_{15}(g')$ differ by ∼1 mag.

While a larger sample with better photometric coverage is still required, we conclude that the 02cx-like class of SNe cannot be well described by a single $M-\Delta m_{15}$ relation. As future time-domain surveys significantly increase the sample of known 02cx-like SNe, it may be the case that further

---

[25] SN 2007qd was first detected after g'-band maximum, which is why it was excluded from the sample in Foley et al. (2013). However, the 50-day range for the time of maximum for SN 2007qd in Table 5 of Foley et al. (2013) ignores the deep upper limits reported in McClelland et al. (2010) between ∼10 and 20 days prior to SN 2007qd's first detection. As argued in McClelland et al. (2010), the initial detection of SN 2007qd is very likely near the epoch of g'-band maximum.

subdivision of the 02cx-like class yields a subset that can be described by a simple $M-\Delta m_{15}$ relation.

5.2. The Relative Rate of 02cx-like SNe to SNe Ia

The controlled nature of the Color Me Intrigued experiment enables a unique estimate of the relative rate of 02cx-like SNe compared to SNe Ia. Assuming that 02cx-like SNe peak at $M \approx -15$ mag, iPTF, which has a detection limit of $R_{PTF} \leqslant 20.5$ mag (Law et al. 2009), can detect these sources to a distance modulus $\mu = 35.5$ mag, corresponding to redshift $z \leqslant 0.03$. We spectroscopically classified all transients discovered during Color Me Intrigued with a known host galaxy with $z \leqslant 0.03$. Below this redshift limit, there were three SNe Ia and one 02cx-like SN, iPTF 16fnm, discovered during the course of the Color Me Intrigued experiment. Under the assumption of observational completeness, we therefore find that the relative rate of 02cx-like SNe to SNe Ia, $r_{02cx/Ia}$, is $1/3 \approx 33\%$.

Prior to estimating the uncertainty on $r_{02cx/Ia}$, we caution that our assumption of observational completeness for 02cx-like SNe during the Color Me Intrigued experiment is likely overly optimistic. First, the luminosity function (LF) of 02cx-like SNe is poorly constrained. If the LF is heavily weighted toward extremely faint 08ha-like SNe, iPTF would have missed any of these beyond $z \approx 0.02$. Second, despite the high-cadence observations during Color Me Intrigued, the ∼week-long gaps in monitoring around full moon could have resulted in additional 02cx-like SNe that were missed. Third, our machine-learning candidate identification software, realbogus, is limited by the flux contrast between the host galaxy and the SN. iPTF is complete to transients that are $>10\times$ brighter than the underlying host surface brightness, but when the contrast drops to $0.7\times$ ($0.2\times$) the host galaxy surface brightness, the completeness drops to ∼50% (∼2%), resulting in missed transients (Frohmaier et al. 2017). These concerns should not affect SNe Ia, which are more luminous and long-lived, meaning that our $z \leqslant 0.03$ sample is potentially biased against 02cx-like SNe. Thus, the rate estimates included here are likely underestimates. Nevertheless, we proceed under the assumption that iPTF detected all $z \leqslant 0.03$ 02cx-like SNe during the Color Me Intrigued experiment.

Following the analysis presented in White et al. (2015), we can calculate confidence intervals for the relative rate of 02cx-like SNe to SNe Ia. Given an outcome with probability p, the chances of getting k successes in a sample of n trials is given by the binomial distribution probability mass function:

$$Pr(k; n, p) = \binom{n}{k} p^k (1 - p)^{n-k}. \quad (1)$$

Assuming a uniform prior [0,1], the probability of p being less than some fiducial value p_0 given an observed fraction k/n is

$$Pr(p < p_0; n, k) = \frac{\int_0^{p_0} Pr(k; n, p) dp}{\int_0^1 Pr(k; n, p) dp}. \quad (2)$$

From here, it follows that the probability that the relative rate $r_{02cx/Ia}$ is less than r_0 given N_{02cx} 02cx-like SNe and N_{Ia} SNe Ia is

$$Pr_{N_{02cx}, N_{Ia}}^{rel}(r_{02cx/Ia} < r_0) = Pr\left(p < \frac{r_0}{1 + r_0}; N_{SN}, N_{02cx}\right), \quad (3)$$

where $N_{SN} = N_{Ia} + N_{02cx}$.

Considering SNe within the 02cx-like volume-limited sample (i.e., $z \leqslant 0.03$), we have $N_{Ia} = 3$ and $N_{02cx} = 1$. We find $Pr_{1,3}^{rel}(r < 190\%) = 95\%$ and $Pr_{1,3}^{rel}(r < 8\%) = 5\%$, which corresponds to a 90% confidence interval for the relative rate of $33_{-25}^{+158}\%$. In this case, small number statistics result in an estimate of the relative rate that is not particularly constraining. Nevertheless, it is consistent with previous estimates, including ∼5% from Li et al. (2011), 5.6% from White et al. (2015), and 31% from Foley et al. (2013). While the methodologies differ, there is general agreement within the (large) uncertainties. Additionally, Li et al. note that their rate is likely underestimated if the LF of 02cx-like SNe extends significantly fainter than SN 2005hk. Given that there are now many known 02cx-like SNe fainter than SN 2005hk (e.g., SN 2008ha, SN 2007qd, SN 2010ae, iPTF 16fnm), it stands to reason that the true rate is likely higher than the estimate in Li et al. After limiting the survey volume to very nearby SNe, Foley et al. (2013) and White et al. (2015) apply correction factors of 2 and 1, respectively, to their relative rate measurements. The factor of 2 adopted in Foley et al. is highly uncertain, given the poorly constrained LF of 02cx-like SNe and the many heterogeneous surveys used to define their sample of 02cx-like SNe. Meanwhile, the assumption that PTF was spectroscopically complete for slow-speed SNe, which is adopted in White et al., is likely overly optimistic. The true value of r^{rel} is likely between 0.05 and 0.3, and future surveys with large volumetric survey speeds (Bellm 2016), such as ZTF, are needed to significantly reduce the uncertainty on this measurement.

6. A Selection Function for 02cx-like SNe: $g' - r'$ Color Evolution

In Foley et al. (2013), the color evolution of 02cx-like SNe is examined to see whether all 02cx-like SNe can be described by a single color curve following a reddening correction, similar to the Lira law for normal SNe Ia (Lira 1996; Phillips et al. 1999). Foley et al. apply reddening corrections to a sample of six 02cx-like SNe and find a significant reduction in scatter for the $V - R$ and $V - I$ color curves. The same corrections do not reduce the $B - V$ scatter, however. As a result, they cannot conclude whether the observed scatter is the result of dust reddening or intrinsic differences in the class.

Here, we instead examine the color curves of 02cx-like SNe as a possible selection function to separate them from normal SNe Ia. While 02cx-like SNe do not follow an $M-\Delta m_{15}$ relation, we find that the $g' - r'$ color evolution is relatively uniform for the class. In Figure 9, we show the $g' - r'$ color evolution for nine 02cx-like SNe: SN 2008ha (Stritzinger et al. 2014), SN 2010ae (Stritzinger et al. 2014), SN 2007qd (McClelland et al. 2010), SN 2005hk (Phillips et al. 2007), SN 2009ku (Narayan et al. 2011), PS1-12bwh (Magee et al. 2017), SN 2015H (Magee et al. 2016), SN 2012Z (Stritzinger et al. 2015), and iPTF 16fnm (where we are using g_{PTF} and R_{PTF} from this study as a proxy for g' and r', respectively). Figure 9 also shows the color evolution of 35 normal SNe Ia and 9 underluminous, 91bg-like SNe Ia from Folatelli et al. (2013). Normal SNe Ia are defined as those spectroscopically classified as normal both by the SuperNova IDentification package (SNID; Blondin & Tonry 2007) and via the method developed in Wang et al. (2009). 91bg-like SNe are defined as those classified as 91bg-like by SNID.
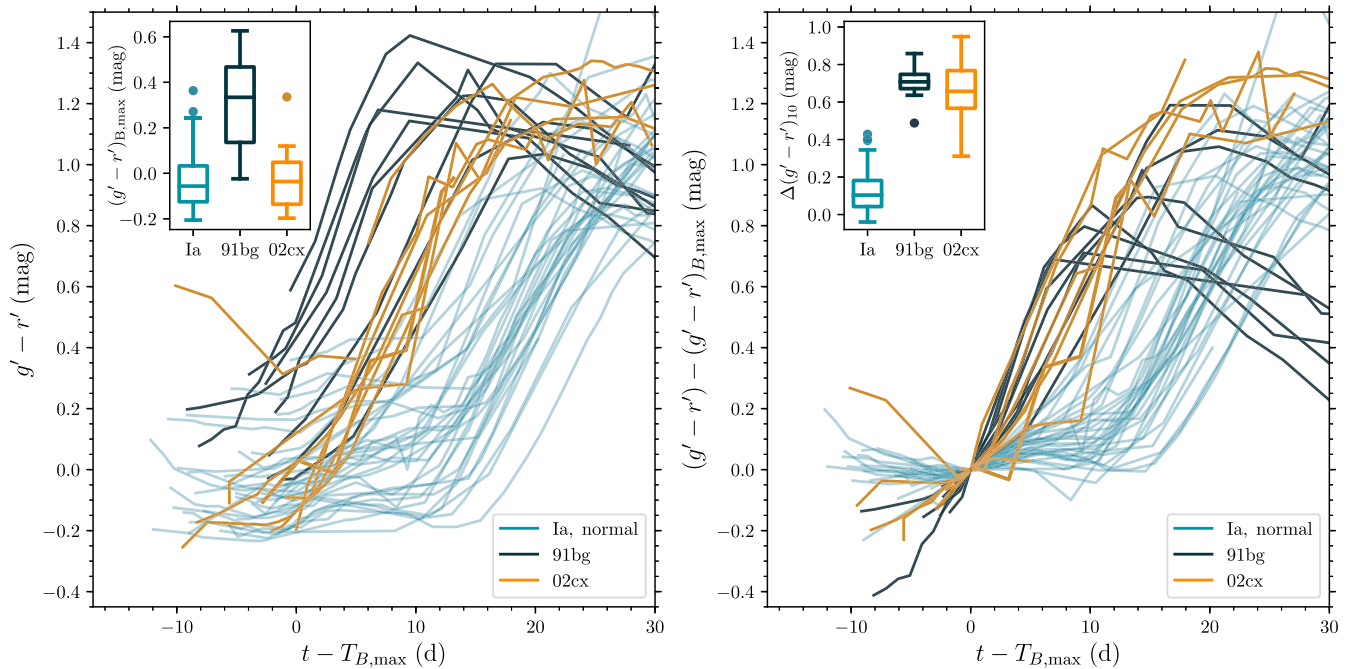
Figure 9. Color evolution of normal (shown in light blue), 91bg-like (dark gray), and 02cx-like (orange) SNe Ia. For clarity, photometric uncertainties are not shown, and the individual measurements are connected via solid lines. The color curves are normalized to $T_{B,\max}$, where available (see text). The color curves are corrected for Galactic extinction, and in some cases host-galaxy extinction as well (see text). The samples for each subclass are defined in the text. The 02cx-like SN 2009ku and SN 2010ae feature gaps in their $g' - r'$ color curves from $\sim+5$ to $+30$ days and from $\sim+11$ to $+45$ days, respectively (Narayan et al. 2011; Stritzinger et al. 2014). As such, we only display these color curves through $+5$ and $+11$ days, respectively. Left: $g' - r'$ color evolution of SNe Ia. The 02cx-like SNe form a remarkably tight sequence with blue colors ($g' - r' \lesssim 0$ mag) at peak and a rapid decline relative to normal SNe Ia. SN 2009ku, which has $g' - r' \approx 0.6$ mag at -10 days, stands out as an outlier relative to the other 02cx-like SNe. The inset shows an interquartile range (IQR) box plot comparing the $g' - r'$ color at $T_{B,\max}$, determined via linear interpolation between the two epochs spanning $T_{B,\max}$, for the three subclasses. SN 2015H is excluded, as the $g' - r'$ color is not available prior to $+6$ days (Magee et al. 2016). At peak, 02cx-like SNe are very blue (the red tail of the distribution is dominated by SN 2009ku), like normal SNe Ia, while 91bg-like SNe are red. Right: color evolution relative to the color at $T_{B,\max}$, denoted here as $(g' - r') - (g' - r')_{B,\max}$. By normalizing relative to the color at $T_{B,\max}$, we track the color evolution independent of line-of-sight extinction. The color at B maximum is determined via linear interpolation (see above). Both 91bg-like and 02cx-like SNe rapidly evolve to the red along a relatively tight sequence, independent of the color at peak. The inset IQR box plot shows the change in $(g' - r')$ color between $T_{B,\max}$ and $+10$ days, $\Delta(g' - r')_{10}$. The box plot clearly confirms that normal SNe Ia remain blue longer than 91bg-like and 02cx-like SNe. SN 2009ku is excluded from the box plot, as there is no $(g' - r')$ measurement at $+10$ days (Narayan et al. 2011).

The light curves in Figure 9 have been normalized to the time of B-band maximum. For three (two) 02cx-like SNe, SN 2007qd, PS1-12bwh, and iPTF 16fnm (SN 2009ku and SN 2015H), the time of g'-band (r'-band) maximum is used as a proxy because B-band observations are not available. Galactic reddening corrections have been applied to all light curves in Figure 9 using the Schlafly & Finkbeiner (2011) updates to the Schlegel et al. (1998) dust maps. The following host-galaxy reddening corrections have also been applied: $E(B - V) =$ 0.09 mag (Phillips et al. 2007), 0.50 mag (Stritzinger et al. 2014), 0.20 mag (Magee et al. 2017), and 0.07 mag (Stritzinger et al. 2015) for SN 2005hk, SN 2010ae, PS1-12bwh, and SN 2012Z, respectively. The remaining five 02cx-like SNe do not show evidence of Na I D absorption at the redshift of the host galaxy (Foley et al. 2009; McClelland et al. 2010; Narayan et al. 2011; Magee et al. 2016), and we therefore make no corrections for host-galaxy reddening. Host-galaxy reddening corrections are not applied to the normal and 91bg-like SNe Ia, as they are not available. As a result, there is likely some excess scatter in the curves traced by both the normal and 91bg-like SN Ia samples in Figure 9.

The relatively tight locus for 02cx-like color evolution, shown in the left panel of Figure 9, reveals a previously unknown characteristic of the class. At peak, 02cx-like SNe are very blue similar to normal SNe Ia (see the left box plot in

Figure 9). While the blue color of 02cx-like SNe near maximum light has clearly been established (e.g., Foley et al. 2013), the tight scatter, $\sim$0.2 mag, in $g' - r'$ at all epochs in the first $\sim$20 days after peak suggests a common evolution.

Similar to the correlation between ejecta velocity and luminosity first noted by McClelland et al. (2010), SN 2009ku stands out as a clear outlier from the majority of the 02cx-like class. To bring SN 2009ku in line with the rest of the 02cx-like sample would require a host-galaxy reddening of $E(B - V) \approx$ 0.35 mag, which would, in turn, make SN 2009ku $\sim$1.2 mag brighter in the g' band. In this scenario, SN 2009ku would be as luminous as, or more luminous than, many normal SNe Ia. As the sample of 02cx-like SNe grows, the similarity of SN 2009ku to the rest of the class should be closely monitored to determine whether SN 2009ku belongs to a new subclass of low-velocity SNe Ia, separate from the other 02cx-like objects.

In addition to following a nearly uniform color curve, 02cx-like SNe exhibit unique $g' - r'$ evolution when compared to normal and 91bg-like SNe Ia. The right panel of Figure 9 shows the change in $g' - r'$ color relative to $g' - r'$ at $T_{B,\max}$. This normalization enables a measurement of the color evolution that is independent of line-of-sight extinction. It shows that 02cx-like and 91bg-like SNe become significantly redder in the first $\sim$10 days after maximum, while normal SNe Ia exhibit nearly constant $g' - r'$ color in the same time frame.

Table 3
Color Selection Results for 02cx-like SNe

SN Type	$(g' - r')_{\mathrm{B,max}}, \Delta(g' - r')_{10}$			
	0.0, 0.5[a]	0.1, 0.4[a]	0.15, 0.4[a]	0.15, 0.3[a]
Normal Ia	0/35	2/35	2/35	4/35
91bg-like	0/9	2/9	3/9	3/9
02cx, obs.[b]	3/8	4/8	5/8	5/8
02cx, dered.[c]	4/8	6/8	6/8	7/8

Notes. Sources bluer than the $(g' - r')_{\mathrm{B,max}}$ cut and with a decline greater than the $\Delta(g' - r')_{10}$ cut are selected as candidate 02cx-like SNe. Our sample includes nine 02cx-like SNe, but SN 2015H is excluded owing to a lack of $(g' - r')_{\mathrm{B,max}}$ measurement. SN 2009ku, which has $(g' - r')_{\mathrm{B,max}} \approx 0.34$ mag, is the only 02cx-like SNe that is not selected by any of the above cuts.
[a] Respective cuts on $(g' - r')_{\mathrm{B,max}}$ and $\Delta(g' - r')_{10}$, in mag.
[b] Recovered 02cx-like SNe when host-galaxy reddening corrections are not applied.
[c] Recovered 02cx-like SNe following host-galaxy reddening corrections, as shown in Figure 9.

To measure this difference, we define the change in $g' - r'$ color between maximum and $+10$ days, $\Delta(g' - r')_{10}$. The right inset in Figure 9 shows that 91bg-like and 02cx-like SNe have similar $\Delta(g' - r')_{10}$ values, while normal SNe Ia have smaller $\Delta(g' - r')_{10}$ values. This, taken in combination with the $g' - r'$ color at peak, provides an empirical method for selecting 02cx-like SNe. At the time of maximum 02cx-like SNe are blue, like normal SNe Ia and unlike 91bg-like SNe, yet they exhibit large $\Delta(g' - r')_{10}$ values, similar to 91bg-like SNe and unlike normal SNe Ia.

The $g' - r'$ color evolution of 02cx-like SNe has important implications for future surveys, such as ZTF and LSST. Spectroscopic completeness will be impossible for these surveys, but it will be possible to identify 02cx-like SNe from their $g' - r'$ color evolution alone. Using our sample of 9 02cx-like SNe, 9 91bg-like SNe, and 35 normal SNe Ia, we summarize the number of each that would be selected following hard cuts on $(g' - r')_{\mathrm{B,max}}$ and $\Delta(g' - r')_{10}$ in Table 3. While we generally advocate against hard cuts for target selection or classification (e.g., Miller et al. 2012), they illustrate the separation of the 02cx-like class in this case.

Table 3 shows that 02cx-like SNe are readily separated based on their $g' - r'$ evolution. For instance, adopting cuts of 0.0 and 0.5 (first column of Table 3) selects a pure sample of 02cx-like SNe, though less than half of the sample is recovered. Relaxing the cuts to 0.15 and 0.4 (third column) recovers more than half of the 02cx-like candidates, while still severely restricting the number of false positives.

Using the relative rate of 02cx-like SNe to normal SNe Ia, 33% (see Section 5.2), and the relative rate of 91bg-like SNe to normal SNe Ia, 19% (Li et al. 2011), we can estimate how many SNe would be selected by these cuts in a volume-limited sample. In a fixed volume with 100 normal SNe Ia we expect to find 19 91bg-like SNe and 33 02cx-like SNe. If we apply cuts of 0.15 and 0.4 on $(g' - r')_{\mathrm{B,max}}$ and $\Delta(g' - r')_{10}$, respectively, we would select $100 \times 2/35 \approx 6$ normal SNe Ia, $19 \times 3/9 \approx 6$ 91bg-like SNe, and $33 \times 5/8 \approx 21$ 02cx-like SNe. This corresponds to a completeness of ~ 0.63 and a precision of ~ 0.63. We caution that this example relies on uncertain rates (Section 5.2) and the assumption that our

sample of SNe is representative of what would be found in a volume-limited survey. Starting next year, ZTF will significantly reduce the uncertainties on both these assumptions. Nevertheless, this selection function for 02cx-like SNe will enable the efficient use of resources in the near future when transients are plentiful and follow-up scarce.

7. Summary and Conclusions

Maximizing information content while maintaining a large discovery rate is a challenge for modern wide-field time-domain surveys. This challenge will only be exacerbated in the coming years as extremely large field-of-view (ZTF) and large-aperture (LSST) surveys come online. The looming orders-of-magnitude increase in discovered transients will overwhelm existing follow-up facilities and generate a "follow-up problem." Ultimately this means that survey telescopes will provide the sole observations of a majority of transients discovered in the coming decade. This near-future reality necessitates the immediate development of photometric-only methods for studying SNe and other transients.

To address the "follow-up problem" in the context of ZTF, we recently completed the Color Me Intrigued experiment during the final semester of iPTF. Color Me Intrigued searched for transients simultaneously in the g_{PTF} and R_{PTF} filters, marking the first time this was done in PTF/iPTF. Color Me Intrigued was designed to reduce the "follow-up problem" for ZTF in two ways: (i) provide templates for the $g_{\mathrm{PTF}} - R_{\mathrm{PTF}}$ colors for transients at the epoch of discovery, which will help inform ZTF follow-up prioritization, and (ii) ensure that color information is available at all epochs. As all PTF/iPTF surveys require two observations per field per night to reject asteroids, Color Me Intrigued provided a significant addition of information without a loss in survey area.

During the course of Color Me Intrigued, we discovered iPTF 16fnm, a new member of the 02cx-like subclass of SNe Ia. iPTF 16fnm peaked at $M_{g_{\mathrm{PTF}}} = -15.09 \pm 0.17$ mag and declined by ~ 1.2 mag in 13 days. The spectra of iPTF 16fnm were emblematic of the 02cx-like class, including the following properties: (i) very low velocity ejecta ($v_{\mathrm{ej}} \approx 3000$ km s^{-1}), (ii) strong absorption from intermediate-mass and Fe-group elements, and (iii) a not fully nebular appearance several months after peak luminosity. Based on its photometric and spectroscopic evolution, iPTF 16fnm is an unambiguous member of the 02cx-like class.

We additionally compared iPTF 16fnm to other 02cx-like SNe and find that it is among the least luminous members of the class. iPTF 16fnm is the second-faintest known SN Ia, after SN 2008ha, which peaked at $M_{g'} = -14.01 \pm 0.14$ mag (Stritzinger et al. 2014).[26] The post-peak spectra of iPTF 16fnm exhibit a striking resemblance to those of SN 2007qd and SN 2010ae, with similar velocities and chemical compositions. These two SNe also peaked at $M \approx -15$ mag, and they exhibit a similar light-curve evolution to iPTF 16fnm. The nearly identical evolution of these three SNe suggests a common origin.

Many studies have looked for correlated properties (luminosity, ejecta velocity, decline rate, etc.) to see whether 02cx-like SNe can be described as a single-parameter family, similar to normal

---

[26] Small changes in the reddening corrections or distance moduli to SN 2007qd or SN 2010ae could shuffle the order of the second, third, and fourth least luminous SNe Ia.

SNe Ia. We update the previous work of White et al. (2015) and find that, at best, there is a weak correlation with large scatter between M and Δm_{15} in both the g' and r' bands. We also examine the $g' - r'$ color evolution of 02cx-like SNe and compare it to normal and 91bg-like SNe Ia. We find that 02cx-like SNe exhibit unique color evolution: blue colors at peak with large $\Delta(g' - r')_{10}$ values. While we do not have a physical explanation for this behavior, this empirical result can be used as a selection function for identifying 02cx-like SNe. We show that simple cuts on $(g' - r')_{B,\mathrm{max}}$ and $\Delta(g' - r')_{10}$ select 02cx-like SNe with high completeness and precision. While limited by small number statistics, we nevertheless measure the relative rate of 02cx-like SNe to normal SNe Ia and find $r_{N_{02cx}/N_{Ia}} = 33^{+158}_{-25}\%$. This measurement is consistent with other estimates in the literature (Li et al. 2011; Foley et al. 2013; White et al. 2015).

In advance of ZTF, the Color Me Intrigued experiment has demonstrated that nightly observations in different filters can efficiently discover transients. In fact, the general success of this experiment has led to the decision to conduct the 3π ZTF public survey[27] with near-simultaneous g_{ZTF} and r_{ZTF} observations. The experiment also shows the power of closely coupling efficient follow-up resources to survey telescopes. In particular, the SEDm correctly identified iPTF 16fnm as a low-velocity SN, despite its low spectral resolution ($R \approx 100$). Indeed, the SEDm model provides one potential path toward reducing the "follow-up problem" for LSST: low-resolution spectrographs on 4 m class telescopes would enable efficient follow-up for LSST transients with $r' \lesssim 22$ mag.

We close with a recommendation for future time-domain surveys. The search for astrophysical transients provides a fast-moving target where new phenomena are regularly uncovered. These new discoveries often require new observational strategies to efficiently increase the sample size of these rarities. Due to its unique aperture and survey capabilities, early observations from LSST will likely reveal new phenomena.[28] If the LSST observational strategy is fixed without flexibility from the start of the survey, then the transient discoveries in year 2 will look like those from year 1, while year 3 will look like year 2, and so on. This scenario is detrimental for the exploration of explosive systems. By emphasizing a change in cadence at periodic intervals, iPTF was able to specifically target rare sources identified by PTF (e.g., the extensive use of a 1-day cadence to find more young SNe similar to PTF 11kly/ SN 2011fe; Nugent et al. 2011; Bloom et al. 2012a; Cao et al. 2016b), while also enabling new methods of exploration, such as Color Me Intrigued. Thus, we advocate for the adoption of some measure of flexibility in the observational strategy of LSST. Even if minor, this flexibility may prove crucial to better understanding the nature of its early discoveries of unusual sources.

ORCID iDs

A. A. Miller ◉ https://orcid.org/0000-0001-9515-478X
M. M. Kasliwal ◉ https://orcid.org/0000-0002-5619-4938
Y. Cao ◉ https://orcid.org/0000-0002-8036-8491
S. Knežević ◉ https://orcid.org/0000-0003-1416-8069
R. Lunnan ◉ https://orcid.org/0000-0001-9454-4639
F. J. Masci ◉ https://orcid.org/0000-0002-8532-9395
P. E. Nugent ◉ https://orcid.org/0000-0002-3389-0586
D. A. Perley ◉ https://orcid.org/0000-0001-8472-1996
T. Petrushevska ◉ https://orcid.org/0000-0003-4743-1679
R. M. Quimby ◉ https://orcid.org/0000-0001-9171-5236
U. D. Rebbapragada ◉ https://orcid.org/0000-0002-2560-3495
J. Sollerman ◉ https://orcid.org/0000-0003-1546-6615
S. R. Kulkarni ◉ https://orcid.org/0000-0001-5390-8563

References

Astier, P., Guy, J., Regnault, N., et al. 2006, A&A, 447, 31
Barbary, K., Dawson, K. S., Tokita, K., et al. 2009, ApJ, 690, 1358
Bellm, E. C. 2016, PASP, 128, 084501
Ben-Ami, S., Konidaris, N., Quimby, R., et al. 2012, Proc. SPIE, 8446, 844686
Blondin, S., & Tonry, J. L. 2007, ApJ, 666, 1024

---

[27] ZTF is a public–private partnership with 40% of the telescope time dedicated to a public survey. The public survey will monitor the full sky observable with P48 with a 3-day cadence.

[28] To highlight a PTF example, commissioning observations led to the discovery of three superluminous SNe (Quimby et al. 2011). The Quimby et al. result established a new class of stellar explosion, while also explaining the nature of SCP 06F6 (Barbary et al. 2009), the most mysterious optical transient known at that time.

Bloom, J. S., Kasen, D., Shen, K. J., et al. 2012a, ApJL, 744, L17
Bloom, J. S., Richards, J. W., Nugent, P. E., et al. 2012b, PASP, 124, 1175
Brink, H., Richards, J. W., Poznanski, D., et al. 2013, MNRAS, 435, 1047
Cao, Y., Kulkarni, S. R., Gal-Yam, A., et al. 2016a, ApJ, 832, 86
Cao, Y., Kulkarni, S. R., Howell, D. A., et al. 2015, Natur, 521, 328
Cao, Y., Nugent, P. E., & Kasliwal, M. M. 2016b, PASP, 128, 114502
Chambers, K. C., Magnier, E. A., Metcalfe, N., et al. 2016, arXiv:1612.05560
Cook, D. O., Kasliwal, M. M., Van Sistine, A., et al. 2017, AAS Meeting, 229, 237.08
Filippenko, A. V. 1997, ARA&A, 35, 309
Fink, M., Kromer, M., Seitenzahl, I. R., et al. 2014, MNRAS, 438, 1762
Folatelli, G., Morrell, N., Phillips, M. M., et al. 2013, ApJ, 773, 53
Foley, R. J., Brown, P. J., Rest, A., et al. 2010, ApJL, 708, L61
Foley, R. J., Challis, P. J., Chornock, R., et al. 2013, ApJ, 767, 57
Foley, R. J., Chornock, R., Filippenko, A. V., et al. 2009, AJ, 138, 376
Frohmaier, C., Sullivan, M., Nugent, P. E., Goldstein, D. A., & DeRose, J. 2017, ApJS, 230, 4
Gal-Yam, A., Arcavi, I., Ofek, E. O., et al. 2014, Natur, 509, 471
Ganeshalingam, M., Li, W., Filippenko, A. V., et al. 2012, ApJ, 751, 142
Hillebrandt, W., Kromer, M., Röpke, F. K., & Ruiter, A. J. 2013, FrPhy, 8, 116
Ivezić, Ž, Tyson, J. A., Acosta, E., et al. 2008, arXiv:0805.2366
Jha, S., Branch, D., Chornock, R., et al. 2006, AJ, 132, 189
Jones, D. O., Scolnic, D. M., Riess, A. G., et al. 2017, ApJ, 843, 6
Kasliwal, M. M. 2011, PhD thesis, California Institute Technology
Kasliwal, M. M. 2012, PASA, 29, 482
Kessler, R., Marriner, J., Childress, M., et al. 2015, AJ, 150, 172
Kromer, M., Fink, M., Stanishev, V., et al. 2013, MNRAS, 429, 2287
Kulkarni, S. R. 2013, ATel, 4807
Kulkarni, S. R. 2016, AAS Meeting, 227, 314.01
Law, N. M., Kulkarni, S. R., Dekany, R. G., et al. 2009, PASP, 121, 1395
Li, W., Filippenko, A. V., Chornock, R., et al. 2003, PASP, 115, 453
Li, W., Leaman, J., Chornock, R., et al. 2011, MNRAS, 412, 1441
Lira, P. 1996, MS thesis, Univ. Chile

Magee, M. R., Kotak, R., Sim, S. A., et al. 2016, A&A, 589, A89
Magee, M. R., Kotak, R., Sim, S. A., et al. 2017, A&A, 601, 62
Masci, F. J., Laher, R. R., Rebbapragada, U. D., et al. 2017, PASP, 129, 014002
Mazzali, P. A., Röpke, F. K., Benetti, S., & Hillebrandt, W. 2007, Sci, 315, 825
McClelland, C. M., Garnavich, P. M., Galbany, L., et al. 2010, ApJ, 720, 704
Miller, A. A., Cao, Y., Piro, A. L., et al. 2017, ApJ, in press (arXiv:1708.07124)
Miller, A. A., Richards, J. W., Bloom, J. S., et al. 2012, ApJ, 755, 98
Moriya, T., Tominaga, N., Tanaka, M., et al. 2010, ApJ, 719, 1445
Mould, J. R., Huchra, J. P., Freedman, W. L., et al. 2000, ApJ, 529, 786
Narayan, G., Foley, R. J., Berger, E., et al. 2011, ApJL, 731, L11
Nugent, P. E., Sullivan, M., Cenko, S. B., et al. 2011, Natur, 480, 344
Ofek, E. O., Laher, R., Law, N., et al. 2012, PASP, 124, 62
Oke, J. B., Cohen, J. G., Carr, M., et al. 1995, PASP, 107, 375
Oke, J. B., & Gunn, J. E. 1982, PASP, 94, 586
Perlmutter, S., Aldering, G., Goldhaber, G., et al. 1999, ApJ, 517, 565
Phillips, M. M. 1993, ApJL, 413, L105
Phillips, M. M., Li, W., Frieman, J. A., et al. 2007, PASP, 119, 360
Phillips, M. M., Lira, P., Suntzeff, N. B., et al. 1999, AJ, 118, 1766
Poznanski, D., Gal-Yam, A., Maoz, D., et al. 2002, PASP, 114, 833
Quimby, R. M., Kulkarni, S. R., Kasliwal, M. M., et al. 2011, Natur, 474, 487
Riess, A. G., Filippenko, A. V., Challis, P., et al. 1998, AJ, 116, 1009
Schlafly, E. F., & Finkbeiner, D. P. 2011, ApJ, 737, 103
Schlegel, D. J., Finkbeiner, D. P., & Davis, M. 1998, ApJ, 500, 525
Shappee, B. J., Prieto, J. L., Grupe, D., et al. 2014, ApJ, 788, 48
Stritzinger, M. D., Hsiao, E., Valenti, S., et al. 2014, A&A, 561, A146
Stritzinger, M. D., Valenti, S., Hoeflich, P., et al. 2015, A&A, 573, A2
Valenti, S., Pastorello, A., Cappellaro, E., et al. 2009, Natur, 459, 674
Wang, X., Filippenko, A. V., Ganeshalingam, M., et al. 2009, ApJL, 699, L139
Wegner, G., Haynes, M. P., & Giovanelli, R. 1993, AJ, 105, 1251
White, C. J., Kasliwal, M. M., Nugent, P. E., et al. 2015, ApJ, 799, 52
Yaron, O., & Gal-Yam, A. 2012, PASP, 124, 668